PROCEEDINGS OF SCIENCE

Lepton flavor in Higgs boson decays

Ka Wa Ho on behalf of the ATLAS and CMS Collaborations[a,*]

[a] *University of Notre Dame,*
Notre Dame, IN 46556, USA

E-mail: kho2@nd.edu

This proceeding reports a selection of recent experimental results on the Higgs boson couplings with charged fermions. These results are published by the ATLAS and the CMS experiments based on a proton-proton collision dataset at $\sqrt{s}$ = 13 TeV with an integrated luminosity of about 138 fb^{-1} collected during Run 2 of the LHC. The first part are results on the Standard Model predicted decays of the Higgs boson to a pair of opposite-charged, same-flavor fermions. These include the first evidence of the $H \to \mu\mu$ decay and constraints on the $H \to ee$ and $H \to c\bar{c}$ decays. The second part focuses on the searches for the lepton flavor violating decays of the Higgs boson, including $H \to \mu\tau$, $H \to e\tau$, and $H \to e\mu$.

21st Conference on Flavor Physics and CP Violation (FPCP 2023)
29 May - 2 June 2023
Lyon, France

*Speaker

PoS(FPCP2023)032

1. Introduction

Couplings of the Higgs boson (H) with (charged) fermions have been studied extensively by the ATLAS [1] and the CMS [2] experiments at the LHC since the discovery [3–5]. In particular, couplings of H with the third generation charged fermions, including t, b, and τ, have been observed and measured to be consistent with the Standard Model (SM) prediction [6, 7]. Recently, there is also significant progress on the search for the H decays to a pair of opposite charged, first or second charged generation fermions of the same flavor. This proceeding reports on these results obtained from a proton-proton (pp) collision dataset at $\sqrt{s}$ = 13 TeV with an integrated luminosity of about 138 fb^{-1} collected during Run 2 of the LHC. The first evidence of $H \to \mu\mu$ is established by the CMS experiment and measured to be consistent with the SM prediction [8]. Fig. 1 shows the combined fit of the H couplings to various SM particles relative to the SM predictions (κ) as a function of their mass, as measured by the ATLAS [6] (left) and the CMS [7] (right) experiments. These fits are carried out with the full Run 2 dataset assuming no invisible or undetected beyond-the-SM (BSM) H decays. It could be seen in both plots that the H couplings are, thus far, consistent to the SM. Although the SM predicted $H \to ee$ and $H \to c\bar{c}$ decays are not observed so far, the constraints on the upper limit of their branching ratios ($\mathcal{B}$) are improved significantly by the dedicated analyses of the full Run 2 dataset [9–12].

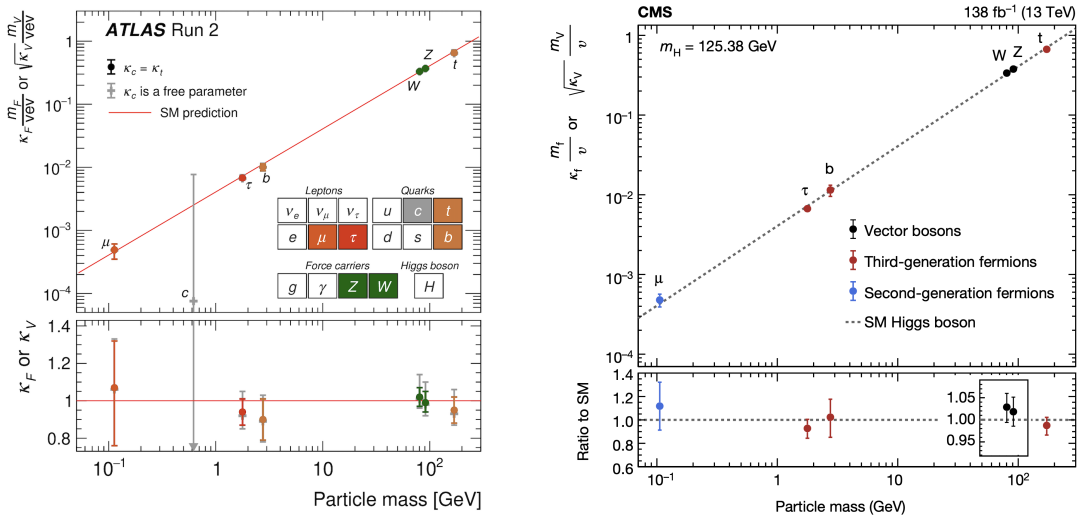

Figure 1: The measured H couplings to various SM particles relative to the SM predictions (κ) as a function of their mass measured with the full Run 2 dataset collected by the ATLAS (left) and the CMS (right) experiments [6, 7]. The couplings modifiers shown are scaled by the corresponding fermionic mass (m_f) or heavy gauge boson mass (m_V) of the particle and the vacuum expectation value (v) of the Brout–Englert–Higgs mechanism to keep a linear proportionality to the particle mass. The values are obtained from a combined fit of H couplings, assuming no invisible or undetected BSM decays of H.

Lepton flavor violation (LFV) decays of H can arise in BSM scenarios through the non-diagonal Yukawa matrices [13]. Dedicated searches for $H \to \mu\tau$, $H \to e\tau$, and $H \to e\mu$ have been carried out by both the ATLAS and the CMS experiments [9, 14–16]. In addition, LFV decays could also arise from potential additional Higgs bosons (X) in the Type-III two Higgs doublet model [17]. Hence, the CMS experiment has also carried out a search for $X \to e\mu$ for a X with a mass (m_X)

within a range 110 – 160 GeV [16]. The upper m_X limit of the search range is set to be below twice the W mass at 160 GeV, where the on-shell decay of $X \to WW$ opens up and becomes dominant [18].

2. Higgs boson flavor

2.1 First evidence of $H \to \mu\mu$

The search for $H \to \mu\mu$ decay by the ATLAS [19] and the CMS experiments [8] make use of the three dominant production modes of H at the LHC, including the gluon-gluon fusion (ggH), the vector boson fusion (VBF), H production in association with a vector boson (ZH and WH), and in association with a top pair ($t\bar{t}H$). Both the ggH and VBF production modes are dominated by the Drell-Yan (DY) backgrounds. For the ZH and WH modes, both analyses focus on the vector boson final states of $Z \to ll$ and $W \to l\nu_l$, where $l = e, \mu$. These production modes are dominated by the WW and WZ diboson backgrounds. For the $t\bar{t}H$ mode, the ATLAS analysis focuses on the fully- and semi-leptonic decays of t while the CMS considers also the hadronic final state of t. The $t\bar{t}$ and $t\bar{t}Z$ processes are the dominant backgrounds in this production mode.

The general strategy of the analyses is to search for a dimuon invariant mass ($m_{\mu\mu}$) resonance at around the H mass (m_H) of 125 GeV. Dedicated boosted decision trees (BDTs) are trained in each signal region (SR) of the analyses targeting the different production modes. Events are then categorized by the BDT scores to separate regions of different expected signal purity. The expected signal shape in each category is modelled via Monte Carlo (MC) simulations. The backgrounds are estimated by carrying a signal-plus-background ($S + B$) parametric fit to the $m_{\mu\mu}$ spectrum of the data directly. This approach applies to all channels of the analyses with the exception of the VBF channel in the CMS analysis, where a deep neural network (DNN), instead of BDTs, is trained to identify signal-like events. The signal strength of $H \to \mu\mu$ is then measured with a maximum likelihood (ML) fit to the DNN score of the simulated signal and backgrounds to the data.

The CMS experiment reports an observed (expected) excess of 3.0 (2.5)σ significance over the expected backgrounds. A combination with the pp collision dataset at $\sqrt{s} = 7$ and 8 TeV during Run 1 of the LHC, corresponding to an integrated luminosity of 5.1 and 19.7 fb^{-1}, gives a measured $H \to \mu\mu$ signal strength of $1.19^{+0.40}_{-0.39}(\text{stat})^{+0.15}_{-0.14}$ (syst) relative to the SM prediction. This establishes the first evidence of $H \to \mu\mu$ in agreement with the SM prediction. The ATLAS experiment also reports an observed (expected) excess of 2.0 (1.7)σ significance over the expected backgrounds. The best fit of the signal strength is reported to be $1.2 \pm 0.6(\text{stat})^{+0.2}_{-0.1}(\text{syst})$ relative to the SM prediction. Fig. 2 [8, 19] shows the $m_{\mu\mu}$ distribution of the data and the corresponding $S + B$ fit, combining all analysis categories of the CMS (left) and the ATLAS experiments (right). The data and the fit in the CMS (ATLAS) figure are weighted by $S/(S+B)$ ($\ln(1 + S/B)$), where S and B are the fitted number of signal and background events, for an illustration of the small signal yield.

2.2 Search for $H \to ee$

The SM predicted branching ratio of $H \to ee$ decay is around 5×10^{-9} while only around 8 million of H are produced during the Run 2 of the LHC [7]. A direct search for $H \to ee$ is

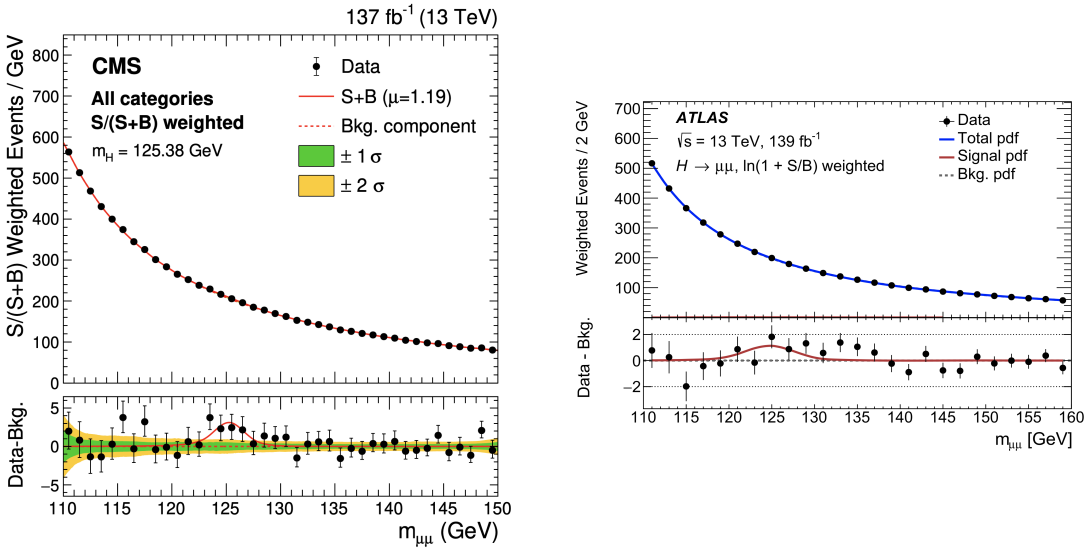

Figure 2: The $m_{\mu\mu}$ distribution of the data and the $S + B$ fit of the CMS (ATLAS) $H \to \mu\mu$ analysis is shown in the upper panel on the left (right), combining all analysis categories. The data and the fit are weighted by $S/(S + B)$ ($\ln(1 + S/B)$) in the CMS (ATLAS) plot, where S and B are the fit number of signal and background events. The lower panels show the residual data events after subtraction by the background component of the $S + B$ fits.

hence expected to be very challenging but its expected branching ratio could also be enhanced in some BSM scenarios [20–22]. Both the ATLAS and CMS experiments have carried out dedicated searches for $H \to ee$ from the two dominant production modes of H, the ggH and the VBF modes [9, 10]. Backgrounds of the searches are dominated by the DY, $t\bar{t}$, and diboson events.

The search strategy of $H \to ee$ is similar to $H \to \mu\mu$, i.e. a search for a dielectron invariant mass m_{ee} resonance at around 125 GeV. The CMS analysis trains a separate BDT for a ggH and a VBF-enriched SR to categorize events according to their expected signal purity. The ATLAS experiment instead categorizes events in a ggH and a VBF-enriched SR in accordance to the transverse momenta (p_T) and the detected pseudo-rapidities (η) of the final state electrons to separate categories of different m_{ee} resolution. The expected signal shape in each category of both analyses is modelled from MC simulations and the backgrounds are estimated directly from data with a $S + B$ parametric fit to the m_{ee} distribution.

An observed (expected) upper limit at 95% confidence level (CL) on the branching ratio of $H \to ee$ decay is set by the CMS collaboration to be $3.0\ (3.0) \times 10^{-4}$, an order of magnitude of improvement relative to the previous result published by CMS experiment based on the pp collision dataset collected during Run 1 of the LHC at $\sqrt{s} = 8$ TeV with an integrated luminosity of 19.7 fb^{-1}. For the ATLAS experiment, the observed (expected) 95% CL limit is set to be $\mathcal{B}(H \to ee) < 3.6\ (3.5) \times 10^{-4}$, which is the first result on $H \to ee$ published by the ATLAS experiment.

2.3 Search for $H \to c\bar{c}$

The search for $H \to c\bar{c}$ decay, having a SM expected branching ratio of around 2.89%, is very challenging in the hadronic environment of the LHC. Both the ATLAS and the CMS experiments have published results on the search for $H \to c\bar{c}$ from the ZH and WH production modes [11, 12]. Both searches focus on the leptonic decays of $Z \to ll$, $Z \to \nu\nu$, and $W \to l\nu_l$, where $l = e, \mu$. Dominating backgrounds in this search are $t\bar{t}$ and W/Z + jets events.

The CMS experiment employs two different search strategies according to the p_T of the reconstructed H. For the "merged-jet" strategy, the H candidate is reconstructed as a single anti-k_T (AK) jet [23, 24] with a cone size of 1.5 with $p_T > 300$ GeV. The H candidate is identified with a dedicated $c\bar{c}$ tagger and a ML fit of the H reconstructed mass is performed to measure the signal yield in this case. Otherwise, the H is reconstructed as two AK4 jets with a cone size of 0.4 (AK4). Each jet selected is required to have a $p_T > 25$ GeV and to pass a dedicated c vs light quark and a c vs b quark tagger. This category is known as the "resolved-jet" category. A ML fit is performed along a dedicated BDT trained in each final state of the associated vector boson to extract the signal strength of $H \to c\bar{c}$.

For the ATLAS experiment, the H candidate is reconstructed from two AK4 jets, with at least one jet passing a dedicated c-tagger and not identified as a b-jet. The reconstructed H candidate is required to have $p_T > 75$ GeV. Events are categorized into 16 SRs according to discriminating kinematics variables against the backgrounds, such as the missing transverse energy (E_{miss}) or the scalar sum of jet transverse momenta (H_T) in each event. 28 additional control regions (CRs) are designed to constrain the $t\bar{t}$, W/Z + jets, and single-top backgrounds. A binned ML fit to the dicharm invariant mass is then carried out to extract the signal strength of $VH(\to c\bar{c})$, $VW(\to c\bar{c})$, and $VZ(\to c\bar{c})$ simultaneously.

A 95% CL observed (expected) upper limit on the signal strength of 14 (7.6) times the SM expectation is reported by the CMS experiment. The analysis strategies are also validated with a first observation of $VZ(\to c\bar{c})$ at a hadron collider in agreement with the SM with a significance of 5.7σ. For the ATLAS experiment, a 95% CL observed (expected) limit on the signal strength of 26 (31) times the SM expectation is reported. This result is a factor of 5 of improvement relative to the previous search at ATLAS with the pp collision data at $\sqrt{s} = 13$ TeV with an integrated luminosity of 36.1 fb^{-1}.

3. Search for lepton flavor violating decays

3.1 $H \to \mu\tau$ and $H \to e\tau$

For both the ATLAS and CMS experiments, the $H \to \mu\tau$ and $H \to e\tau$ decays searches [14, 15] focus on the two dominant production modes of H, the ggH and VBF modes. The $H \to \mu\tau$ and $H \to e\tau$ channels are further categorized according to the decay mode of the final state τ. Both the hadronic (τ_h) or the leptonic decay modes (τ_l with $l = \mu, e$) of the τ lepton are considered. In total, four channels: $H \to \mu\tau_h$, $H \to e\tau_h$, $H \to e\tau_\mu$, and $H \to \mu\tau_e$ are considered. The $Z \to \tau\tau$, W + jets, and quantum chromodynamics (QCD) multi-jets processes are the dominant backgrounds of the searches.

Background estimate techniques are used in both analyses to improve the sensitivities of the searches. Instead of fully relying on MC simulations, the CMS analysis estimates backgrounds with a $\tau^+\tau^-$ pair by replacing the μ in the $\mu^+\mu^-$ data events with simulated τs. Backgrounds from jets misidentified as leptons are estimated from dedicated Z + jets enriched CRs for τ_h channels or from same charge CRs of the final state leptons with loosen isolation requirements for τ_l channels. In a similar fashion, the ATLAS analysis estimates misidentified lepton backgrounds from same charge CRs with relaxed isolation requirement on the final state leptons for the τ_l channels. For the τ_h channels, misidentified lepton backgrounds are estimated from W + jets or QCD enriched CRs with relaxed ID requirement on the final state τ_h.

The CMS analysis sets upper limits on $\mathcal{B}(H \to \mu\tau)$ and $\mathcal{B}(H \to e\tau)$ independently with ML fits along the BDTs trained separately for the various analysis categories targeting the ggH or the VBF mode. For the ATLAS analysis, three separate BDTs are trained in the τ_l channels to target different backgrounds of 1) misidentified leptons, 2) single-top, diboson, and $H \to WW$ events, and 3) DY and $H \to \tau\tau$ events. For the τ_h channels, two BDTs are trained to target the $Z \to \tau\tau$ backgrounds or others. An additional BDT is trained for the ggH enriched category in the $e\tau_h$ final state to target the misidentified leptons backgrounds. A ML fit of the combined BDT scores is performed to measure $\mathcal{B}(H \to \mu\tau)$ and $\mathcal{B}(H \to e\tau)$ simultaneously.

No significant excess of $H \to \mu\tau$ or $H \to e\tau$ events are observed. A 95% CL observed (expected) upper limits of $\mathcal{B}(H \to \mu\tau) < 0.15$ (0.15)% and $\mathcal{B}(H \to e\tau) < 0.22$ (0.16)% are reported by the CMS experiment. The ATLAS experiment reports a 95% CL observed (expected) upper limits of $\mathcal{B}(H \to \mu\tau) < 0.18$ (0.09)% and $\mathcal{B}(H \to e\tau) < 0.20$ (0.12)%.

3.2 $H \to e\mu$ and $X \to e\mu$

The searches for $H \to e\mu$ decay by the ATLAS [9] and CMS experiments [16] focus also on the ggH and VBF modes. The search strategy is similar to the $H \to \mu\mu$ and $H \to ee$ searches, i.e. a search for an $e\mu$ invariant mass ($m_{e\mu}$) resonance at around 125 GeV. Separate BDTs are trained for a ggH and a VBF-enriched SR in the CMS analysis to categorize events according to their expected signal purity. The ATLAS experiment categorizes events a ggH and a VBF-enriched SR according to the p_T and the η of the electron-muon pair to separate categories of different $m_{e\mu}$ resolution. A $S + B$ parametric fit to the $m_{e\mu}$ distribution in data is carried out to extract an upper limit of the $H \to e\mu$ branching ratio. The expected signal shapes are approximated from MC simulations in each category. In additional to $H \to e\mu$, the CMS analysis considers also $X \to e\mu$ by a search for a $m_{e\mu}$ resonance with an unknown mass in the range from 110 to 160 GeV.

The observed (expected) 95% CL limit of $H \to e\mu$ is set to be $\mathcal{B}(H \to e\mu) < 4.4$ (4.7) $\times 10^{-5}$ by the CMS experiment and $\mathcal{B}(H \to e\mu) < 6.2$ (5.9) $\times 10^{-5}$ by the ATLAS experiment. For $X \to e\mu$, a global excess of 3.0σ of events over the expected SM backgrounds is reported at $m_X \approx 146$ GeV in the fit range of $m_{e\mu}$ from 100 – 170 GeV. A scan of the 95% CL observed and expected upper limits of the cross section of $pp \to X \to e\mu$ as a function of the hypothesised m_X is shown as Fig. 3 [16]. The observed significance of the excess is insufficient to draw any conclusions and more data will be needed to clarify its nature. Fig. 4 shows the $m_{e\mu}$ distribution of the data and the $S + B$ fit at $m_X \approx 146$ GeV, combining all analysis categories of the CMS analysis [16] on the left. The data and fit are weighted by $S/(S + B)$ to illustrate the small fitted signal yiel. A similar plot for the $H \to e\mu$ search of ATLAS is shown on the right [9].

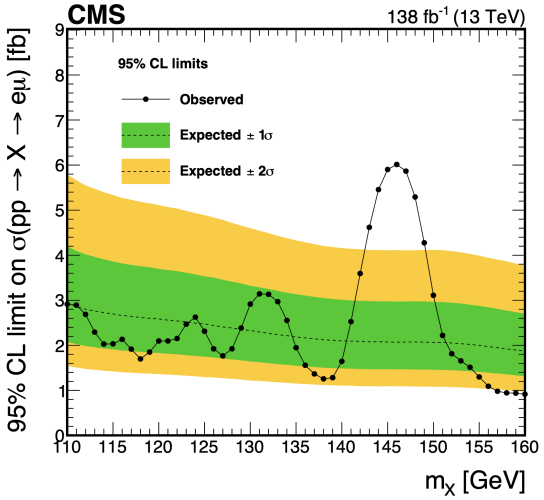

Figure 3: A scan of the 95% observed and expected upper limits of the cross section $\sigma(pp \to X \to e\mu)$ as a function of the hypothesised m_X. The solid (dashed) line shows the observed (expected) upper limits at 95% CL. The green (yellow) band shows the one (two) standard deviation uncertainty in the expected limit.

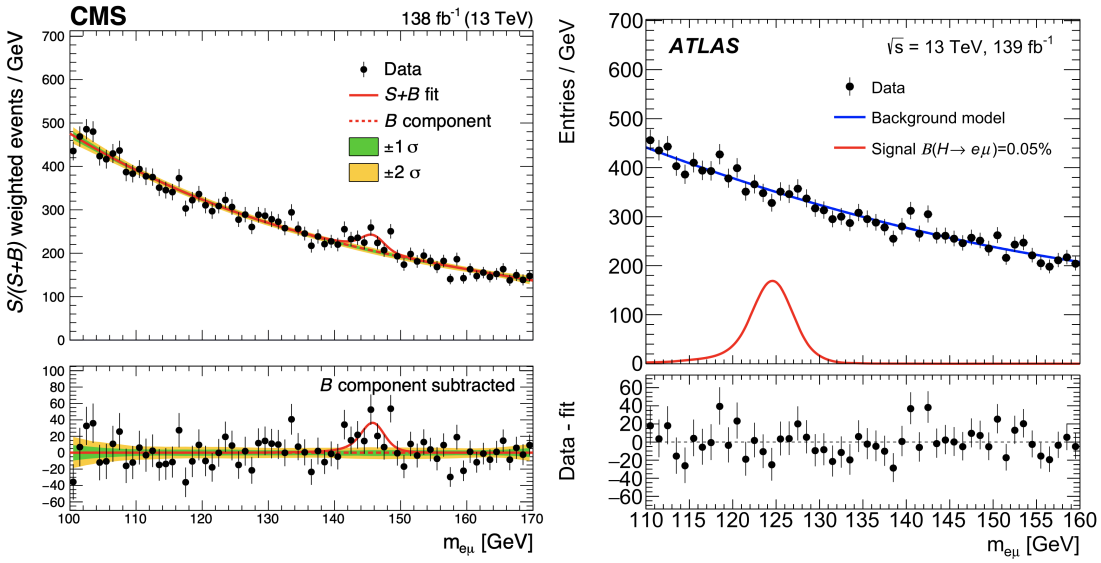

Figure 4: The $m_{e\mu}$ distribution of the data and the $S+B$ fit at $m_X \approx 146$ GeV of the CMS search for $X \to e\mu$ is shown in the upper panel of the left, combining all analysis categories. The data and fit are weighted by $S/(S+B)$ in the plot, where S and B are the fit number of signal and background events. Similarly, the $m_{e\mu}$ distribution of the data, the background, and the signal model of the ATLAS search for $H \to e\mu$ is shown in the upper panel of the right, combining all analysis categories. The lower panel in both plots shows the residual data events after subtraction by the background component of the fits.

4. Conclusion

The couplings of H to the charged fermions of μ, τ, b, and t are measured to be consistent with the SM prediction at both the ATLAS and the CMS experiments. Constraints on the branching ratio of $H \to ee$ and $H \to c\bar{c}$ are improved significantly in both experiments with the full Run 2

dataset collected at the LHC. The direct constraints on the LFV H decays have also improved in all the three channels of $H \to \mu\tau$, $H \to e\tau$, and $H \to e\mu$. An excess of $X \to e\mu$ events of 3.0σ over the expected SM backgrounds is reported by the CMS experiment at $m_X \approx 146$ GeV. The nature of this excess is unclear and will have to be clarified with more data collected.

References

[1] ATLAS Collaboration, "The ATLAS Experiment at the CERN Large Hadron Collider", *JINST* **3** (2008) S08003, doi:10.1088/1748-0221/3/08/S08003.

[2] CMS Collaboration, "The CMS experiment at the CERN LHC", *JINST* **3** (2008) S08004, doi:10.1088/1748-0221/3/08/S08004.

[3] ATLAS Collaboration, "Observation of a new particle in the search for the standard model Higgs boson with the ATLAS detector at the LHC", *Phys. Lett. B* **716** (2012) 1, doi:10.1016/j.physletb.2012.08.020, arXiv:1207.7214.

[4] CMS Collaboration, "Observation of a new boson at a mass of 125 GeV with the CMS experiment at the LHC", *Phys. Lett. B* **716** (2012) 30, doi:10.1016/j.physletb.2012.08.021, arXiv:1207.7235.

[5] CMS Collaboration, "Observation of a new boson with mass near 125 GeV in pp collisions at $\sqrt{s}$ = 7 and 8 TeV", *JHEP* **06** (2013) 081, doi:10.1007/JHEP06(2013)081, arXiv:1303.4571.

[6] ATLAS Collaboration, "A detailed map of Higgs boson interactions by the ATLAS experiment ten years after the discovery", *Nature* **607** (2022) 52, doi:10.1038/s41586-022-04893-w, arXiv:2207.00092.

[7] CMS Collaboration, "A portrait of the Higgs boson by the CMS experiment ten years after the discovery", *Nature* **607** (2022) 60, doi:10.1038/s41586-022-04892-x, arXiv:2207.00043.

[8] CMS Collaboration, "Evidence for Higgs boson decay to a pair of muons", *JHEP* **01** (2021) 148, doi:10.1007/JHEP01(2021)148, arXiv:2009.04363.

[9] ATLAS Collaboration, "Search for the Higgs boson decays $H \to ee$ and $H \to e\mu$ in pp collisions at $\sqrt{s}$ = 13 TeV with the ATLAS detector", *Phys. Lett. B* **801** (2019) 135148, doi:10.1016/j.physletb.2019.135148, arXiv:1909.10235.

[10] CMS Collaboration, "Search for the Higgs boson decay to a pair of electrons in proton-proton collisions at $\sqrt{s}$ = 13 TeV", Technical Report CERN-EP-2022-131, CERN, Geneva, 2022. arXiv:2208.00265, https://cds.cern.ch/record/2823465.

[11] ATLAS Collaboration, "Direct constraint on the Higgs-charm coupling from a search for Higgs boson decays into charm quarks with the ATLAS detector", *Eur. Phys. J. C* **82** (2022) 717, doi:10.1140/epjc/s10052-022-10588-3, arXiv:2201.11428.

[12] CMS Collaboration, "Search for Higgs boson decay to a charm quark-antiquark pair in proton-proton collisions at $\sqrt{s}$ = 13 TeV", *Phys. Rev. Lett.* **131** (2023) 061801, doi:10.1103/PhysRevLett.131.061801, arXiv:2205.05550.

[13] R. Harnik, J. Kopp, and J. Zupan, "Flavor violating Higgs decays", *JHEP* **03** (2013) 026, doi:10.1007/JHEP03(2013)026, arXiv:1209.1397.

[14] ATLAS Collaboration, "Direct constraint on the Higgs-charm coupling from a search for Higgs boson decays into charm quarks with the ATLAS detector", *Eur. Phys. J. C* **82** (2022) 717, doi:10.1140/epjc/s10052-022-10588-3, arXiv:2201.11428.

[15] CMS Collaboration, "Search for lepton-flavor violating decays of the Higgs boson in the $\mu\tau$ and eτ final states in proton-proton collisions at $\sqrt{s}$ = 13 TeV", *Phys. Rev. D* **104** (2021) 032013, doi:10.1103/PhysRevD.104.032013, arXiv:2105.03007.

[16] CMS Collaboration, "Search for the lepton-flavor violating decay of the Higgs boson and additional Higgs bosons in the eμ final state in proton-proton collisions at $\sqrt{s}$ = 13 TeV", Technical Report CERN-EP-2023-061, CERN, Geneva, 2023. arXiv:2305.18106, https://cds.cern.ch/record/2860172.

[17] G. C. Branco et al., "Theory and phenomenology of two-Higgs-doublet models", *Physics Reports* **516** (2012) 1, doi:10.1016/j.physrep.2012.02.002, arXiv:1106.0034.

[18] R. Primulando, J. Julio, and P. Uttayarat, "Collider constraints on lepton flavor violation in the 2HDM", *Phys. Rev. D* **101** (2020) 055021, doi:10.1103/PhysRevD.101.055021, arXiv:1912.08533.

[19] ATLAS Collaboration, "A search for the dimuon decay of the Standard Model Higgs boson with the ATLAS detector", *Phys. Lett. B* **812** (2021) 135980, doi:10.1016/j.physletb.2020.135980, arXiv:2007.07830.

[20] A. Dery, C. Frugiuele, and Y. Nir, "Large Higgs-electron Yukawa coupling in 2HDM", *JHEP* **04** (2018) 044, doi:10.1007/JHEP04(2018)044, arXiv:1712.04514.

[21] W. Altmannshofer, J. Brod, and M. Schmaltz, "Experimental constraints on the coupling of the Higgs boson to electrons", *JHEP* **05** (2015) 125, doi:10.1007/JHEP05(2015)125, arXiv:1503.04830.

[22] G. F. Giudice and O. Lebedev, "Higgs-dependent Yukawa couplings", *Phys. Lett. B* **665** (2008) 79, doi:10.1016/j.physletb.2008.05.062, arXiv:0804.1753.

[23] M. Cacciari, G. P. Salam, and G. Soyez, "The anti-k_t jet clustering algorithm", *JHEP* **04** (2008) 063, doi:10.1088/1126-6708/2008/04/063, arXiv:0802.1189.

[24] M. Cacciari, G. P. Salam, and G. Soyez, "FastJet user manual", *Eur. Phys. J. C* **72** (2012) 1896, doi:10.1140/epjc/s10052-012-1896-2, arXiv:1111.6097.

PoS(FPCP2023)032